Chapter 3: Synthesis and characterization of mycolic acid containing nanoparticles

3.1 Introduction

As described in chapter 1 and 2, MA is a constituent of *M.tb* which forms the major part of the cell wall of the bacteria. MA consists of an extended family of long chain 2-alkyl 3-hydroxyl fatty acids, typically 70-90 carbon atoms in length. The reason why MA was considered as targeting agent is twofold: Firstly as an antigen that forms immune-complexes with anti-MA antibodies, which universally occur in all TB patients [120] and may facilitate opsonisation of the nanoparticles for macrophage uptake mainly at the site of antigen production; and secondly, because of the cholesteroid nature of the MA molecules [121]. By its property of attraction of cholesterol, it may in effect be attracted to the cholesterol rich site of *M.tb* infection. Due to the extremely hydrophobic nature of mycolic acids, a suitable vehicle was needed to introduce them into the body and guide them to their presumed targets of infection. The synthetic PLGA polymer was ideally suited to encapsulate both the MA and the drug into nanoparticles, as they can harbour both hydrophilic as well as hydrophobic molecules.

Nanoparticles are generally prepared with natural or synthetic polymers using various techniques including emulsification, nanoprecipitation and salting out procedures to yield particles ranging in size between 10-1000 nm [29, 35, 36]. These particles were first developed by Birrenbach and Speiser in the 1970's [171]. Nanoparticles, spheres or capsules can be made, depending on the method used and the specific characteristics needed from the particle. Improved efficacy, fewer dosages to be administered due to sustained release properties, reduced toxicity and delivery of therapeutic agents to the site of infection are some of the benefits of nano-encapsulated drugs as discussed in more detail in chapter 1. An additional advantage

of nanocarriers for treatment of intracellular infections such as *M. tb* is their intracellular uptake and accumulation in macrophages, which is also the target of infection of *M.tb* [45, 172].

Nanoparticles have the advantage over other drug carriers such as liposomes or micelles [173] by their increased stability and slow release of drugs. This makes them better to control compared to liposomes, which are generally leaky and with limited shelf life [34]. The sub-micron size of nanoparticles effects a higher cellular uptake and ability to penetrate deep into tissue, therefore being able to target a wider variety of biological components within cells of choice than larger microparticles could [51]. By functionalizing the surface of the particles with a targeting ligand, higher bioavailability is generated at the site of infection and therefore the dose and side effects of the drug may be minimized [51].

For this study it was decided that PLGA nanoparticles will be used as the nanocarrier for the MA and INH drug for reasons explained in Chapter 1. The PLGA nanoparticle carrier was designed to encapsulate MA together with an anti-TB drug, INH, in an attempt to increase the drug's efficacy. The developed formulation was tested on *M.tb* infected macrophages, after the MA containing nanoparticle drug was assembled and tested *in vitro* for uptake by macrophages and cytotoxicity.

A double emulsion solvent evaporation technique was used for formation of the particles. They were characterized for Zeta potential, a measure of surface charge, dynamic light scattering, i.e. size analysis and size distribution, and surface morphology. The latter was investigated by means of scanning electron microscopy (SEM). The drug and lipid encapsulation efficiency was measured spectrophotometrically. For effective therapy and usefulness of the polymer drug construct the intracellular uptake and trafficking *in vitro* of the particles were investigated. The THP-1 and U937 monocyte-macrophage-like cell lines were used. Cellular uptake of fluorescently labelled nanoparticles was assessed with confocal laser scanning microscopy. The cytotoxicity of the nanoparticles was investigated by the WST and MTT technologies, i.e. cell proliferation assays.

3.2 Hypothesis

The antigenic, cholesteroid nature of free mycolic acids of *M.tb* can be exploited by their inclusion into INH-containing nanoparticles to facilitate uptake of the nanoparticles into TB infected macrophages.

3.3 Aims of study

- Encapsulation and characterization of the product of natural mycolic acids in biodegradable polymers.
- Encapsulation and characterization of the product of natural mycolic acids together with an anti-TB drug isoniazid.
- Analysis of the intracellular uptake of the mycolic acid containing nanoparticles by means of co-localization studies with organelle specific markers
- Performing toxicity tests on mycolic acid containing nanoparticles to confirm the safety of use of MA as targeting agent as well as testing the efficacy of the isoniazid encapsulated nanoparticles together with mycolic acids.

3.4 Materials

3.4.1 Consumables

Acetic acid	Saarchem, Gauteng, RSA (Unilab)
Alexa fluor 488:	
chicken anti-mouse IgG (H+L)	Invitrogen, Oregon USA

Alexa fluor 633:	
Goat anti-mouse IgG (H+L)	Invitrogen, Oregon USA
Alexa Fluor 633:	
Rabbit anti-mouse IgG (H+L)	Invitrogen, Oregon USA
BACTEC 460 culture media	Becton Dickinson International, Belgium
Basic fuchsin	Fluka, Sigma-Aldrich, Steinheim, Germany
5-Bromomethyl fluorescein	Molecular Probes, Leiden, The Netherlands
Calcium chloride	Merck, Darmstadt, Germany
Chloroform	Merck, Darmstadt, Germany
Cytochalasin D	Sigma Chemical Co., St Louis, USA
Dakocytomation fluorescent	
mounting medium oil	Dako Cytomation, Carpentaria, CA, USA
Dextran Alexa Fluor 647,	
10 000 MW, anionic, fixable	Invitrogen, Oregon, USA
Dichloromethane	Merck, Darmstadt, Germany
Dimethyl sulfoxide	Sigma Chemical Co., St Louis, USA
3(4,5-dimethylthiazol-2)-2,5-diphenyl	
tetrazolium bromide (MTT)	ICN Biomedicals, Ohio, USA
DMEM culture media	Highveld biologicals, RSA
Dynasore	Sigma Chemical Co., St Louis, USA
Ethanol	BDH, Gauteng, RSA (Analytical grade)
5-N-ethyl-N-isopropylamiloride	

(EIPA)	Sigma Chemical Co., St Louis, USA
Foetal calf serum	Highveld biologicals, RSA
Ferrous oxide nanoparticles	Gift from prof. Walter Focke, University of Pretoria, SA
Hexane	Merck, Darmstadt, Germany
Isoniazid, 99% purity	Sigma Aldrich, Steinheim, Germany
Magnesium chloride	Merck, Darmstadt, Germany
Methyl-β-cyclodextran	Sigma Chemical Co., St Louis, USA
Monoclonal anti-α-Tubulin antibody produced in mouse	Sigma Chemical Co., St Louis, USA
Mycolic acids	Sigma Chemical Co., St Louis, USA
Nocodazole	Sigma Chemical Co., St Louis, USA
Paraformaldehyde	Merck, Darmstadt, Germany
Penicillin/Streptomycin	Highveld biologicals, RSA
Phalloidin-Tetramethyl rhodamine B Isothiocyanate	Sigma Chemical Co., St Louis, USA
Phenol	BDH, Gauteng, RSA
Phorbol 12-myristate 13-acetate	Sigma Chemical Co., St Louis, USA
Poly, DL, lactic-co-glycolic acid, 50:50 (Mw: 45000-75000)	Sigma Chemical Co., St Louis, USA
Polyvinyl alcohol (PVA) MW: 13000-23000,	

partially hydrolysed (87-89)	Sigma Chemical Co., St Louis, USA
Sodium chloride	Saarchem, Gauteng, RSA
di-Sodium hydrogen phosphate	Merck, Darmstadt, Germany
Potassium chloride	Merck, Darmstadt, Germany
Potassium dihydrogen phosphate	Merck, Darmstadt, Germany
RPMI-1640 culture media	
(with L-glutamine)	Gibco, Invitrogen, Paisley, UK
Silica Oxide (amorphous)	Gift from prof. Walter Focke, University of Pretoria, SA
Sodium dodecyl sulphate	Sigma Chemical Co., St Louis, USA
Transferrin Alexa Fluor 633	Invitrogen, Oregon, USA
Triton X-100	Sigma Chemical Co., St Louis, USA
Trypan blue	Sigma Chemical Co., St Louis, USA
Trypsin/ Versene	Highveld biologicals, RSA
Wortmannin	Sigma Chemical Co., St Louis, USA
Zinc oxide nanopowder	Sigma Chemical Co., St Louis, USA

3.4.2 Buffers

PBS buffer (PBS): 8.0 g NaCl, 0.2 g KCl, 0.2 g KH_2PO_4 and 1.05 g Na_2HPO_4 per 1 L double distilled, deionized water, adjusted to pH 7.4

Buffer A: PBS containing 1mM $CaCl_2$ and 1mM $MgCl_2$

3.4.3 Instrumentation

Size and zeta potential measurements: Zetasizer nano-zs, Malvern instruments, Worcstershire, UK.

Confocal microscopy: Leica TCS SP5 confocal microscope, Mannheim, Germany.

Morphology of particles was investigated on a LEO 1525 Field Emission SEM.

For particles synthesis and characterization: Silverson L4R homogenizer, UK,

Virtis Benchtop freeze dryer, USA.

Absorbancies were measured with a SLT 340 ATC photometer.

FACS analysis: Becton Dickinson FACS ARIA Cell Sorter, USA.

In vitro mycobacterial growth experiments: BACTEC 460 radiometric apparatus, Becton Dickinson, Johnston Laboratories, USA.

3.5 Methods

3.5.1 Preparation of INH containing nanoparticles with labelled MA

To prepare nanoparticles, the double emulsion solvent evaporation freeze drying technique was used as previously described in literature with modifications [174]. Poly DL, lactic-co-glycolic acid (PLGA) 50:50 (MW: 45000-75000) was dissolved in 6 ml of dichloromethane (DCM) at a concentration of 1.25% weight/volume (w/v). Partially labelled MA (1:1 w/w, with 5-Bromomethylfluorescein (5BMF) labelled MA total of 2 mg, 1.7 µmol) was dissolved in 2 ml dichloromethane and added whilst stirring. For the first water in oil (w/o) emulsion, aqueous phosphate buffer saline (PBS, pH 7.4, 2 ml) was added to the mixture and homogenization was done at 5000 rpm for 3 min. For nanoparticles containing INH, the INH (100 mg, 729 µmol) was

dissolved in the PBS and then added to the mixture. The emulsion formed was subsequently transferred to an aqueous solution of 1% w/v of the polyvinyl alcohol (PVA, MW: 13000-23000 and partially hydrolysed (87-89%)) as a stabilizer. The second water in oil in water (w/o/w) emulsion was formed by homogenization at 8000 rpm for 3 min. The second emulsion formed was stirred at 500 rpm overnight at atmospheric pressure to evaporate the organic solvent. The PLGA nanoparticles were recovered by centrifugation at 19000 rpm for 15 min. The resulting particles were dried by lyophilization in a Vitrus Benchtop freeze dryer.

3.5.2 Nanoparticle characterization

The nanoparticles collected after lyophilization was subjected to size distribution, polydispersity and surface potential measurements by means of a zetasizer. The samples were diluted with PBS and manually shaken to disperse the particles into solution before measurement at a temperature of 25 °C. The surface morphology of the particles was investigated by scanning electron microscopy done by the Nano Centre department at the CSIR. The gold sputtering technique was used to prepare the samples for visualization by fixing the NPs to aluminum sample stubs with double-sided carbon tape and sputter coating with gold for viewing by scanning electron microscopy. Drug and lipid loading was analyzed as described in the subsequent sections.

3.5.2.1 Quantification of INH in nanoparticles

Quantification of the INH encapsulated in the nanoparticles was performed via an indirect method. The supernatant left after particle centrifugation was tested for the amount of free INH present in the supernatant measured with absorbance at 260 nm. The amount of drug was calculated by the formula:

Equation 1:

$$\text{Encapsulation efficiency (EE)} = \frac{\text{Amount of drug initially used} - \text{amount of drug in the supernatant}}{\text{Amount of drug initially used}} \times 100$$

3.5.2.2 Quantification of MA in nanoparticles

For the MA-containing nanoparticles, carbol fuchsin dye (basic fuchsin 0.3 g, ethanol (95%) 10.0 ml, phenol 5.0 ml, ddd H_2O 95 ml) was used to quantify the amount of MA present in the nanoparticles. The MA containing nanoparticles (20 mg) were dissolved in chloroform (10 ml) and stirred overnight. Hexane was added to precipitate the PLGA, and stirred vigorously for an hour. The precipitate was recovered by filtration through a 0.45 µm organic solvent resistant filter (Pall Acrodisk, PSF, GXF/GHP) and washed with hexane 2 to 3 times. The mother liquor was evaporated with N_2 (g). The MA left in the vial was re-dissolved in hexane followed by the addition of an equal amount of carbol fuchsin dye. To prepare the standards, MA was dissolved in hexane and added to the Carbol fuchsin (1:1 v/v). The Carbol fuchsin forms a lower pink aqueous layer and MA in hexane forms the upper transparent layer. After thorough mixing the upper layer turned pink due to the complex formation between MA and Carbol fuchsin. The absorbance of the hexane layer was measured at 492 nm in an absorbance plate reader and a standard curve was compiled.

3.5.3 *In vitro* cell viability assay

Caco-2 cells (human colorectal carcinoma) and U937 (histiocytic lymphoma) cells were purchased from Highveld Biologicals, RSA. The cells were grown and maintained at a confluency of 0.5 – 5 x 10^6 cells/ml, in DMEM media for Caco-2 and RPMI-1640 for U937 cells, both supplemented with penicillin (50 µg/ml), streptomycin (50 µg/ml) and 10% heat inactivated foetal calf serum (FCS). The cells were incubated at 37 ºC in a 5% CO_2 (g) humidified incubator and passaged 2-3 times a week. Cell viability was determined by making use of the trypan blue exclusion test.

Cells were seeded in 96 well plates at a density of 0.5 - 1 x 10^6 cells/ml at 100 µl per well and incubated for 24 hours before treatment. U937 cells were differentiated as described in 3.5.4.2. Cells were incubated with different concentrations of empty PLGA nanoparticles, MA nanoparticles or Fluorescein-MA containing nanoparticles of an average size of ~ 500 nm. Ferrous oxide (Fe_2O_3) [175, 176] and amorphous silica oxide (SiO_2) were used as negative controls [177] and zinc oxide (ZnO) nanopowder with known toxicity [178] was used as positive control in the studies in order to determine cell viability after exposure. The WST assay (Quick Cell Proliferation Assay Kit II, Biovision, USA) was performed as per manufacturer's procedures for the Caco-2 cells. The assay is based on the reduction of the tetrazolium salt, WST to water-soluble orange formazan by cellular mitochondrial dehydrogenase present in viable cells. The amount of formazan dye formed is determined colourimetrically at 450 nm with a reference wavelength at 630 nm. It is directly proportional to the number of living cells. The MTT assay was performed for the U937 cells by adding the MTT dissolved in PBS pH 7.4 (100 µg/well) to the cells and incubated for 5 hours at 37 °C. The untransformed MTT was removed by careful aspiration and the formazan crystals formed, were dissolved in 100 µl dimethyl sulfoxide. The absorbance was read at 550 nm. Percentage viability was calculated by the absorbance intensity of the cells incubated with the particles as a function of that of the untreated cells.

3.5.4 Uptake of nanoparticles by macrophages

In order to elucidate the feasibility of these nanoparticles for intracellular delivery of drugs, nanoparticle uptake into macrophage cells *in vitro* was analysed by fluorescence activated cell sorting (FACS).

3.5.4.1 Cell culture maintenance

To determine particle uptake flow cytometry experiments were conducted as follows. For cell growth the THP-1 monocytes were grown in RPMI-1640 medium with L-glutamine, supplemented with penicillin (50 µg/ml), streptomycin (50 µg/ml) and 10% heat inactivated FCS and maintained as described in 3.5.3.

3.5.4.2 Differentiating cells

To differentiate the THP-1 cells into adherent macrophages, 50 nM Phorbol 12-myristate 13-acetate (PMA) was added to the wells containing 1 x 10^6 cells/ml with total volume of 2 ml per well and incubated for 48 hours [172, 179]. Thereafter the medium was replaced with complete RPMI-1640 media for another 24 hours. The formation of adherent macrophages was confirmed via microscopy.

3.5.4.3 Flow cytometry

Differentiated THP-1 cells were washed twice with PBS at room temperature (RT). Thereafter the cells were incubated for 2 hours at 37 °C in incomplete RPMI containing different concentrations of Fluorescein-MA or Rhodamine containing nanoparticles, which were similar in size. The plates containing the cells were subsequently placed on ice and the cells were washed twice with ice cold PBS. Ice cold acid wash (NaCl 1.15 g and Acetic acid 1.14 ml /100 ml) was included and the plates were incubated for 1min. on ice. The cells were then washed twice with PBS at

RT and trypsinized at RT with 600 µl trypsin/versene (0.25 % Trypsin + 0.05 % EDTA). To inhibit the trypsin reaction, 600 µl ice cold PBS was added. The cells were washed twice with ice cold PBS, centrifuged at 900 rcf for 3 min. and resuspended in trypan blue stain to minimize background fluorescence [180, 181]. The cells were washed once more and resuspended in ice cold PBS. The fluorescence of 10 000 viable cells was acquired via the fluorometer.

Chemical uptake inhibitors were used to investigate the mechanism of uptake. The differentiated cells were incubated in incomplete RPMI for 15 min. at 37 °C containing either 150 nM wortmannin, 5 mM methyl-β-cyclodextran, 75 µM dynasore, 10 µM nocodazole, 10 µM 5-N-ethyl-N-isopropylamiloride (EIPA), 50 µM cytochalasin D. Fluorescein-MA or Rhodamine containing nanoparticles were subsequently added and incubated for a total of 2 hours in the continued presence of the inhibitors. The cells were then prepared for FACS analysis as describe above. The specific inhibitors used were wortmannin – affects macropinocytosis and phagocytosis by inhibiting PI(3)kinase, methyl-β-cyclodextran – extracts cholesterol and affects lipid rafts, dynasore is a dynamin GTPase inhibitor, nocodazole depolymerises the microtubule network, 5-N-ethyl-N-isopropylamiloride (EIPA) is used to inhibit macropinocytosis and cytochalasin D depolymerises the actin network [140, 182, 183].

3.5.5 Nanoparticle uptake and localization by confocal microscopy

To determine where the NP's localize within the cells, live and fixed cell imaging was conducted.

3.5.5.1 Cell culture maintenance

For cell growth of the suspension cultures, the THP-1 monocytes and the human monocyte-macrophage like cell line U937 were grown and maintained in RPMI-1640

medium with L-glutamine, supplemented with penicillin (50 µg/ml), streptomycin (50 µg/ml) and 10% heat inactivated foetal calf serum (FCS) and maintained as described in 3.5.3.

3.5.5.2 Differentiating cells

To differentiate the cells into adherent macrophages, THP-1 (1 x 10^6 cells/ml) was exposed to 50 nM PMA whereas the U937 (1 x 10^6 cells/ml) cell line was exposed to 8 nM PMA for 48 hours [179, 184]. Thereafter the medium was replaced with complete RPMI-1640 medium for another 24 hours and the formation of adherent macrophages was confirmed via microscopy. The differentiated cells were treated for live cell imaging or fixed for immunostaining.

3.5.5 3 Nanoparticle uptake in U937 and THP-1 macrophages

In order to determine the uptake of the particles in the macrophage cells, the cells were incubated for an hour with Fluorescein-MA containing PLGA nanoparticles (0.1 mg/ml). The cells were then washed three times with buffer A (PBS containing 1mM $CaCl_2$ and 1mM $MgCl_2$) and visualized in 1 ml of clear incomplete RPMI on the Leica confocal microscope equipped with a temperature stage set at 37 °C.

3.5.5.4 Nanoparticle, transferrin and dextran uptake in U937 and THP-1 macrophage cells

In order to determine the accumulation point of molecules within intracellular compartments a pulse/chase study was conducted. A pulse/chase analysis allows for the determination of the endocytic route of the particles by successively exposing the cells to the labeled particles and/or endosomal marker (pulse) thereafter removing the

excess particles followed by an incubation step (chase) [185]. The study was performed with the nanoparticles together with transferrin, which is a marker of early endosomes and the late endosome marker, dextran. For the THP-1 and U937 macrophages, the media was removed and replaced with incomplete RPMI for 10 min. at 37 °C. The nanoparticle solutions (0.1 mg/ml) suspended in incomplete RPMI were then added to the cells (pulse step), and incubated for 4 hours [186]. Thereafter the cells were washed 3 times with buffer A at 37 °C. Buffer A was replaced with complete RPMI and the cells were incubated for a further 3.5 hours and another 0.5 hours in incomplete RPMI (chase step). To the cells, 100 nM transferrin 633 (final concentration of 0.008 mg/ml) was added and incubated as indicated in table 3.3. The cells were washed 3 times with buffer A at 37°C. Incomplete, clear RPMI (1 ml) was added at 37 °C. The cells were visualized via confocal microscopy equipped with a temperature stage set at 37 °C. Alternatively, instead of transferrin 633, the pulse/chase study was performed with dextran alexa fluor 647 (0.125 mg/ml).

3.5.5.5 Nanoparticle treatment and fixation of macrophage cells

Nanoparticle (0.2 mg/ml in incomplete RPMI) treatment of the cells consisted of a 3 hour incubation followed by washing the cells 3 times in buffer A at room temperature (RT). The fixation medium, 3% PFA (paraformaldehyde) in PBS was added to cover the cells and left for 20 min. The wells were then washed 3 times with buffer A and dipped once in distilled H_2O. The excess water was drained and the coverslip mounted on a glass slide face down together with a drop of Dakocytomation fluorescent mounting medium oil. Subsequently the coverslip was sealed with clear nail polish. Confocal microscopy was then conducted as needed.

3.5.5.6 Immunofluorescence staining of U937 and THP-1 fixed macrophages

To determine the uptake of the nanoparticles by the cells, the cells were treated with Fluorescein-MA PLGA nanoparticles (0.1 mg/ml in incomplete RPMI) for 4 hours at 37 ºC. Thereafter the cells were fixed and stained for α-tubulin with serial antibody treatment. Alternatively cells were incubated for 15 min. with the actin depolymerising agent, Cytochalasin D (5 µM) or the microtubule polymerization disrupting agent, Nocodazole (10 µM) at 37 ˚C in incomplete RPMI. The media was removed and the cells were either washed 3 times with PBS and treated with nanoparticles, or the cells were not washed, but treated with nanoparticles. Another set was treated with Cytochalasin D (5 µM) or Nocodazole (10 µM) at 37 ˚C for a total of 4 hours. Cytochalasin D treated and untreated cells were then stained for actin as described in 3.5.5.6.2. Nocodazole treated and untreated cells were then stained for α-tubulin as described in 3.5.5.6.1.

3.5.5.6.1 Immunostaining for α-tubulin

The medium was removed and the cells washed once with ice cold PBS. Methanol (100%) at –20 ˚C was quickly added (to maintain microtubule integrity) and incubated for 5 min. The rest of the method was done at RT. The cells were washed 3 times in PBS and then a blocking solution (10% FCS in PBS) was added for 30 min. The primary α-tubulin mouse antibody (25 µl of 1:500 dilution in blocking buffer) was added to the cells and incubated for 30 min. at RT. The cells were washed 3 times in 0.2% Triton/PBS and once in PBS only at RT. The secondary anti-mouse antibody (25 µl of 1:400 dilution in blocking buffer) was added and incubated for 45 min. at RT in a humidified atmosphere in the dark. The cells were then washed 3 times in 0.2% Triton/PBS and once in PBS at RT. The cells were washed twice in buffer A at RT and prepared for confocal imaging.

3.5.5.6.2. Rhodamine staining for actin

The cells were fixed with 3% PFA as described in 3.5.5.5 and incubated with Phalloidin-Tetramethyl rhodamine B isothiocyanate (2 µg/ml) for 10 min. at RT. The cells were then washed 4 times with buffer A at RT and prepared for confocal viewing.

3.5.6 *In vitro* drug testing in *Mycobacterium tuberculosis* H37Rv infected THP-1 macrophages

In order to determine what the antimicrobial effect will be on intracellular bacteria, the *M.tb* H37Rv strain was used for drug susceptibility testing in THP-1 macrophages by making use of the radiometric CO_2 (g) - release BACTEC 460 apparatus.

3.5.6.1 Cell culture maintenance

For cell growth THP-1 monocytes (kind gift from Dr. B. Baker from University of Stellenbosch, SA) were grown and maintained as described in 3.5.4.1 but without the addition of antibiotics through out the entire duration of the experiments.

3.5.6.2 Differentiating cells

All the experiments were conducted in the differentiated macrophage state of the cells unless otherwise stated. To differentiate the cells into adherent macrophages, THP-1 (1×10^6 cells/ml) were treated with 100 nM PMA in RPMI/FCS [179, 184]. To ensure monolayer formation the plate was tilted for 1 minute per side and repeated several times. The cells were incubated at 37 ºC in a 5% CO_2 (g) atmosphere for 24 hours. Thereafter the cells were washed twice with RPMI/FCS media and left for another 24 hours. The formation of adherent macrophages was confirmed with microscopy.

3.5.6.3 Macrophage infection with *M.tb* H37Rv

A frozen aliquot of *M.tb* H37Rv was thawed (2.3 X 10^8 CFU/ml) and passaged 30 times up and down with a 1 ml insulin syringe. The amount required (5:1 multiplicities of infection (MOI), thus 5 x 10^6 mycobacteria per well) was centrifuged (520 µl per 24 well plate) at 13 000 rpm for 20 min. The supernatant was removed and 1.2 ml medium (RPMI/ FCS) was added. The bacteria were resuspended in the media by passaging 30 times up and down with 1 ml insulin syringe. To each well of 1 x 10^6 cells, 50 µl of *M.tb* H37Rv was added for infection. The plate was incubated for 4 hours and then washed to remove non-internalized *M.tb* H37Rv, before incubation overnight.

3.5.6.4 Nanoparticle drug treatment

Nanoparticles containing INH and partially labelled MA were prepared in RPMI/FCS medium at a final concentration of 0.2 µg/ml and 2 µg/ml of free INH. After the medium was removed from the wells, 1 ml of the prepared nanoparticle suspensions was added to the cells, and incubated for 5 hrs, 1 day or 2 days with additional 2 day incubation after removing the particles not taken up by the cells [172].

3.5.6.5 Harvesting TB bacilli from macrophages

After the nanoparticle treatment the cells were washed 3 times with RPMI/FCS to remove non-phagocytosed TB bacteria and un-ingested particles. Cells were harvested by removing 1 ml of medium and adding 100 µl 0.25% SDS to each tube, at a final concentration of 0.025%. To the wells 1 ml of 0.025% SDS was added to lyse the adherent macrophages or alternatively 0.1% Triton X-100 was used for this purpose.

The cells were physically removed by gentle pipetting. The suspension of cells was removed and added to tubes. Centrifugation at 13 000 rpm for 20 min. was done to pellet the bacteria. The pellet was passaged 10 times up and down with a 1 ml insulin syringe in 100 µl Bactec 460 media and added to the Bactec vials.

For the controls, drug free vials consisted of bacterial inocula only. Negative control vials contained media without any bacteria or drugs to monitor if any contamination occurred. All the vials were read and flushed with 5% CO_2 (g) daily until the growth index (GI) of the bacterial control reached 999.

3.6 Results

3.6.1 Characterization of MA / INH encapsulated particles

The freeze dried particles, recovered after the encapsulation of INH and MA in the double emulsion evaporation technique [174], were used in all experiments without further purification. The particles were subsequently subjected to size and zeta potential analysis with a Zetasizer. Knowing the zeta potential, the stability of the nanoparticles in terms of aggregation in different media may be predicted. Charged nanoparticles have a lesser tendency to aggregate than neutral nanoparticles. Table 3.1 describes the physical characteristics obtained for the nanoparticles.

Table 3.1. Mean diameter and zeta potential of nanoparticles prepared by the solvent evaporation freeze drying method

Sample	**Average particle size (nm)**	**Polydispersity index (PDI)**	**Zeta potential (mV) in PBS pH 7.4**
PLGA NP	412 (± 82)	0.43	-9.2 (± 0.7)
Fluorescein-MA PLGA	508 (± 101)	0.48	- 5.32 (± 1.8)
50% Fluorescein-MA/MA/ INH/ PLGA	555 (± 86)	0.51	- 6.68 (± 0.2)
INH/PLGA	419 (± 92)	0.47	- 8.39 (± 1.6)

nm = nanometer, mV = milli-volts

The technique reproducibly yielded drug-free nanoparticles of 412 (± 82) nm diameter as well as nanoparticles loaded with MA and INH of 555 (± 86.4) nm, as analyzed by dynamic light scattering. The nanoparticle suspension stability was examined by

measuring the zeta potential. Theoretically, the more positive or negative the values are, the less the possibility for aggregation. PLGA has a negative zeta potential due to the presence of uncapped end carboxyl groups. The values indicated that the MA lipid molecules reduced the negative values to some extent. The change in zeta potential could be an indication that some of the MA molecules may be located on the external surface of the PLGA nanoparticles.

Spectrophotometric determination of the concentration of INH was determined indirectly, by measuring the amount of INH (measured at 260 nm) present in the supernatant after collection and washing of the nanoparticles. The amount of drug encapsulated in the nanoparticles is given in table 3.2.

Table 3.2. Concentration of the INH in the sample

Sample	**Starting mass of INH (mg)**	**Encap-sulation efficiency (EE)**	**Yield (mg)**	**Loading (%)**	**Amount of drug in sample (mg)**
INH/PLGA	96	0.1201	79.4	14.52091	11.5296
50% Fluorescein-MA /MA /INH PLGA	107	0.1135	86.7	14.0075	12.1445

Thus the amount of drug in the sample is approximately 14% of particle mass. The encapsulation efficiency (EE) was determined by using equation 1 from section 3.5.2.1. The encapsulation efficiency indicates the final amount of drug incorporated into the system compared to the original amount of drug used, whereas the percentage drug loading in the sample is the amount of drug in the whole formulation of the nanoparticle samples.

The surface morphology of the formed nanoparticles was characterized via SEM. The SEM was used to study the external morphology of the PLGA nanoparticles. Figure 3.1 shows a micrograph of nanoparticles containing fluorescein-MA NPs magnified 50 000 times. The image shows coalescent, spherical particles with a smooth surface containing no observable pores and a large size distribution as also indicated by the PDI in table 3.1. A variation in size would possibly lead to the individual particles having different release profiles of the drug which is a function of polymer degradation where the smaller particles could degrade faster. The results showed that the external morphology of the particles had a smooth spherical surface which will facilitate more uniform particle degradation. Thus by making use of the double emulsion evaporation freeze drying technique, successful formation of MA containing PLGA nanoparticles was achieved together with the anti-TB drug INH.

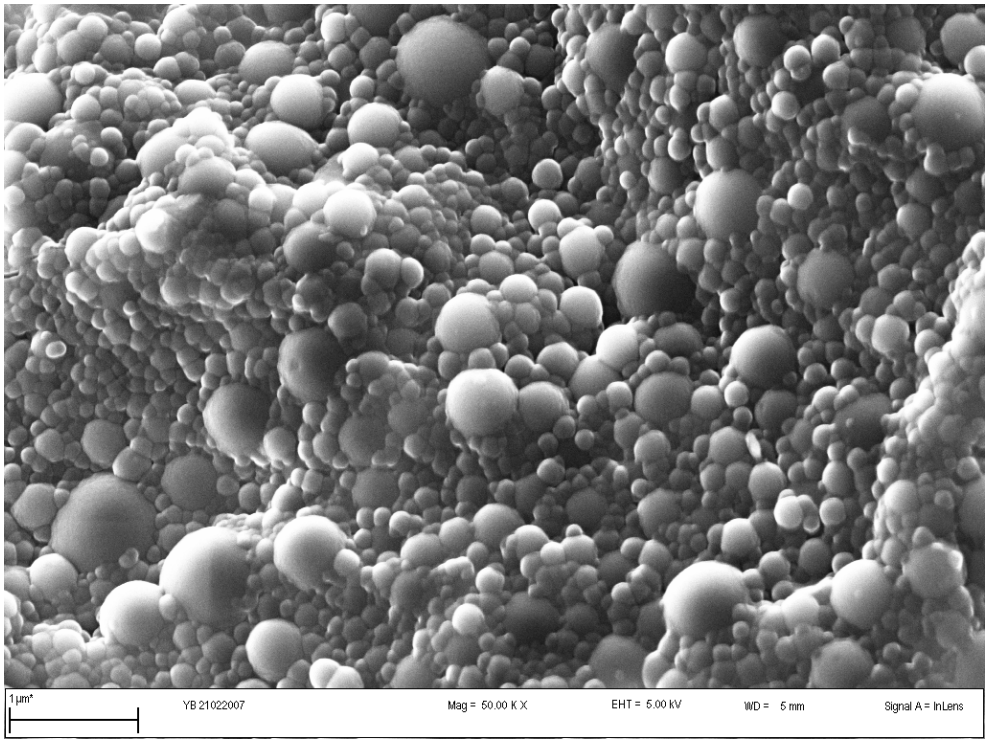

Figure 3.1 *Representative SEM image of the surface of PLGA nanoparticles with Fluorescein labelled MA.*

3.6.2 Quantification of MA containing nanoparticles

MA are long chain 2-alkyl 3-hydroxyl fatty acids comprising typically of 70-90 carbon atoms making it a very hydrophobic molecule with limited solubility in commonly used solvents. Different methods could be employed to determine the encapsulation efficiency into nanoparticles. However, the hydrophobicity of MA limits the techniques that can be used. In literature, HPLC analysis is used for the detection of mycobacterium species through their different mycolic acid profiles [187-190], applying primarily a photodiode array detector. Because mycolic acids do not contain suitable chromophores for UV detection, derivatization is needed for spectrophotometric detection. Another method of quantification is by colorimetric methods. According to a patent by Khanuja S *et al*. published in 2003 [191], mycolic acids could be quantified by making use of a carbol fuchsin dye indicated in Figure 3.2. This dye interacts with the MA in a concentration dependent way, producing a coloured complex that could be measured at 492 nm.

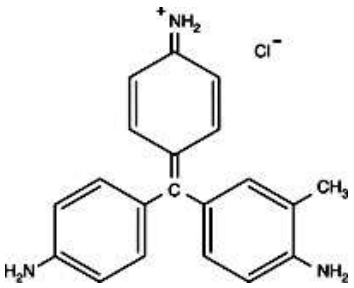

Figure 3.2 *Basic fuchsin that will associate with mycolic acids of M.tb [191].*

From the standard curve prepared, the amount of MA in the sample could be determined. Thus, by making use of the equation obtained for the standard curve (Figure 3.3) for the Fluorescein-MA PLGA particles: 0.5 mg Fluorescein -MA in 73 mg NP sample with an encapsulation efficiency of 26% was observed. PLGA was also tested alone as a control.

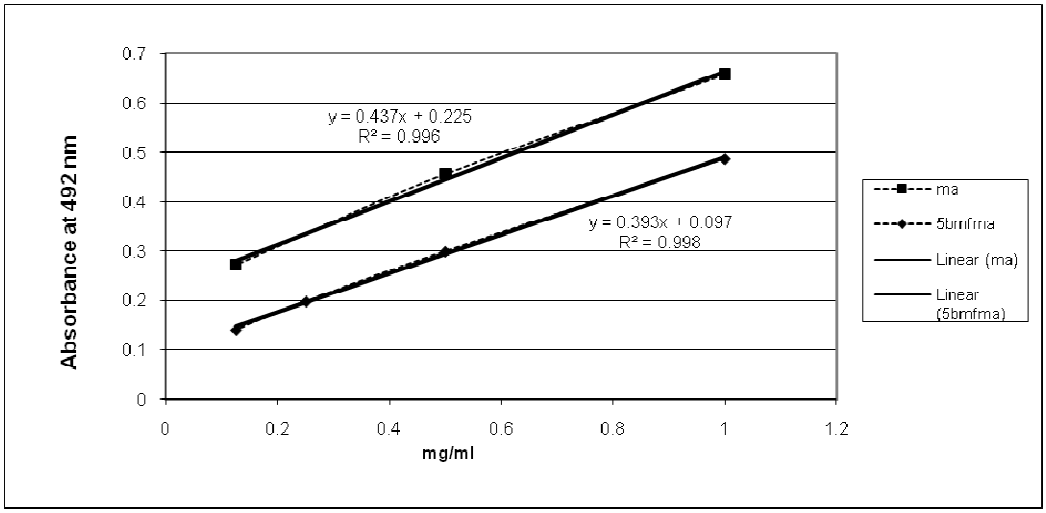

Figure 3.3 *Standard curve obtained for MA and Fluorescein-MA by making use of the Carbol fuchsin dye.*

3.6.3 *In vitro* cell viability assay

In order to elucidate the effect of the nanoparticles on the viability of cells, non-radiometric assays were used to determine *in vitro* the cell viability after treatment with the specific MA containing nanoparticles. By making use of the WST assay, the *in vitro* cytotoxicity of MA containing nanoparticles were compared to PLGA nanoparticles, amorphous SiO_2, Fe_2O_3 particles and ZnO nanopowder at concentrations of 0.1, 0.01 and 0.001 mg/ml. The adherent Caco-2 cells were exposed for 3.5 hours to the different compounds and incubated for a further 20.5 hours. The cells were then washed and incubated in fresh complete media. The results in figure 3.4 indicated that compared to untreated cells (control), the Caco-2 cell lines showed more than 75% viability when treated with various concentrations of PLGA nanoparticles, SiO_2 and Fe_2O_3 particles. Therefore the PLGA nanoparticles compared well to the controls and did not show any adverse effects on the cells. This result illustrates the safety of this drug delivery system. MA containing nanoparticles caused no more than 25% cell death in the Caco-2 cells. MA containing nanoparticles showed lower % viability with statistical significance ($P < 0.01$) compared to PLGA only nanoparticles, whereas the Fluorescein-MA containing nanoparticles compared to PLGA did not differ with significance. The MA containing nanoparticles differed

from the % viability with statistical significance ($P < 0.01$) compared to Fluorescein-MA nanoparticles. One possible reason for this is that the percentage MA in the Fluorescein-MA is less than for the MA alone. The MA (0.01 mg/ml) but not the Fluorescein-MA containing nanoparticles statistically were not significantly more toxic compared to the control, ZnO, but this might be attributed to the large standard deviation obtained for the ZnO. A longer incubation time up to 48 hour and 72 hours study was also done, but because of the fast growth rate of the Caco-2 cells even after treatment, the nanoparticles did not show any significant toxicity in comparison to the controls.

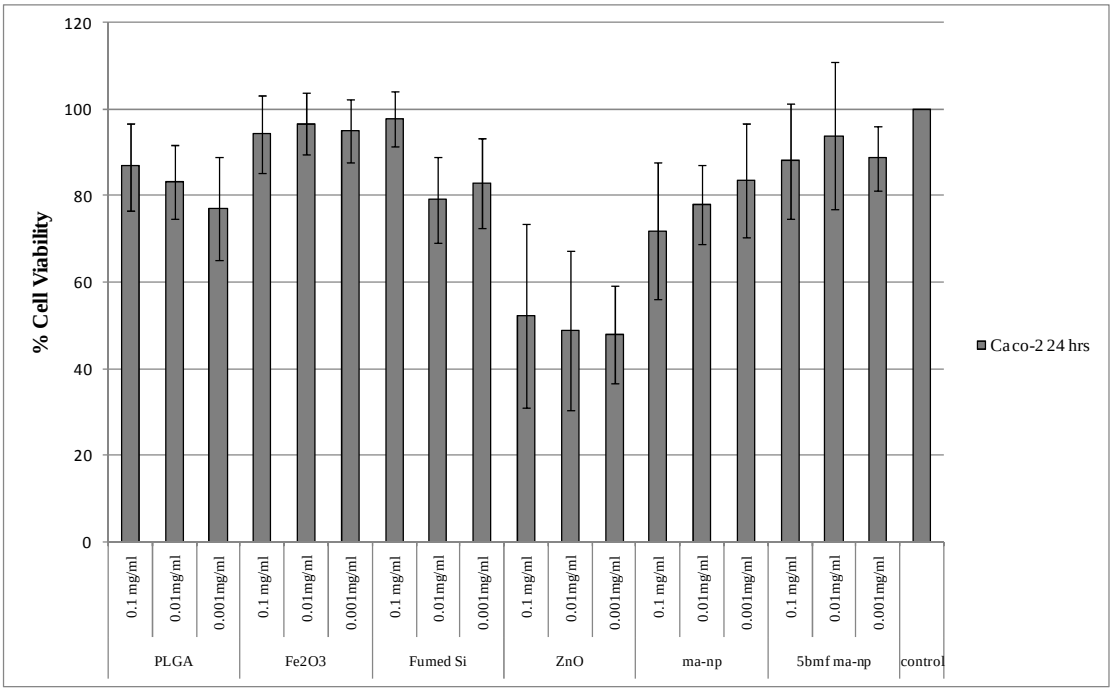

Figure 3.4 *Effects of PLGA, ferrous oxide, fumed silica, zinc oxide and MA containing particles on viability of the Caco-2 cell line after 24 hours as done by a WST assay. The data are representative of two repeats of n = 6 and the error bars indicate standard deviation.*

An initial viability study on differentiated U937 macrophage cells was also done by means of a non-radiometric MTT assay [192, 193]. The formazan crystals formed were dissolved and the absorbance of the dye measured as an indication of the number

of live cells per well. MA containing nanoparticles showed more than 80% viability in the U937 cells as shown in figure 3.5. Because the MTT assay was not repeated statistical significance was not determined. But these initial studies do indicate that the MA containing nanoparticles have a small negative effect on the cell growth albeit a bit more toxic compared to PLGA nanoparticles alone.

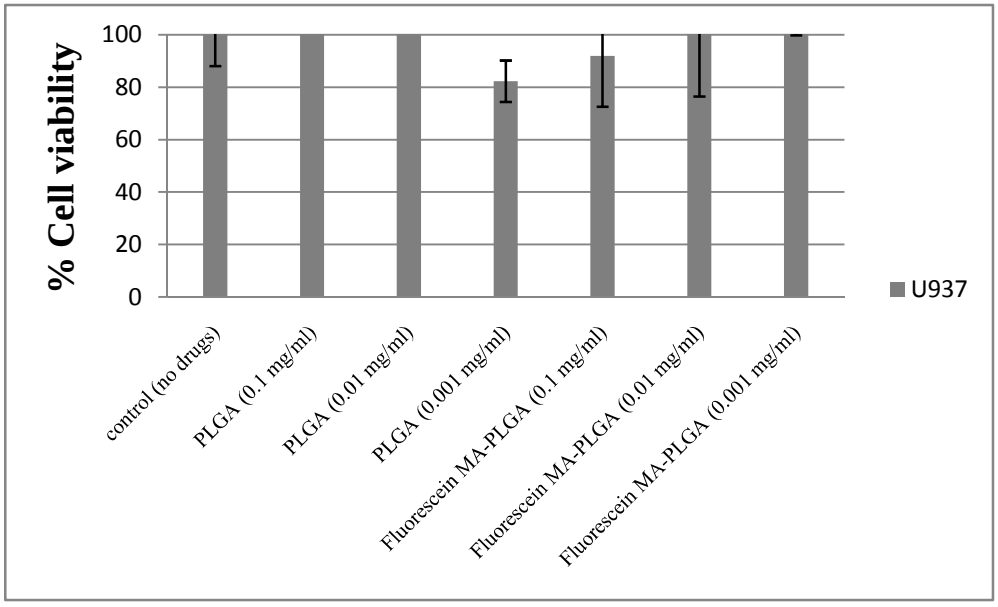

Figure 3.5 *Effects of PLGA and MA containing particles on viability of the U937 cell line after 24 hours as done by a MTT assay. The data are representative of one experiment of n = 4 and the error bars indicate standard deviation.*

3.6.4 Flow cytometric measurement of uptake of nanoparticles by macrophages

The THP-1 cells were used in their chemically differentiated state. Uptake of labelled nanoparticles by macrophages was measured by flow cytometry. The instrument was set for each sample to collect 10 000 events. Fluorescein and rhodamine have excitation wavelengths of 488 nm and 526 nm respectively and were detected at their respective emission wavelengths of 520 nm and 555 nm. The data consisted of side scatter, forward scatter and fluorescence emission centered at 520 nm (P1, for Fluorescein) and 555 nm (P2, for rhodamine). Labelled and unlabelled samples were

used to set the respective gates, where the unlabelled cells would be eliminated from the analyzed population. The Fluorescein-MA and Rhodamine containing nanoparticles of a similar size range were used for this study. In addition cells were washed with a trypan blue solution before analysis to quench extracellular fluorescence, therefore measuring only the fluorescent particles that were internalized [180].

The results shown in figure 3.6 for both of the nanoparticle groups indicate a concentration dependent uptake in macrophage cells. The graphs indicated that no additional fluorescence peaks were observed when the cells were exposed to higher concentrations of MA or rhodamine containing nanoparticles. Thus it could be assumed that only the number of cells that take up the particles are increased and that all cells take up similar amounts of particles. Thus MA seems not to interfere with the thermodynamics of the nanoparticle uptake. For the confocal studies a concentration of 0.1 mg/ml was used, so that the macrophages were not saturated with nanoparticles.

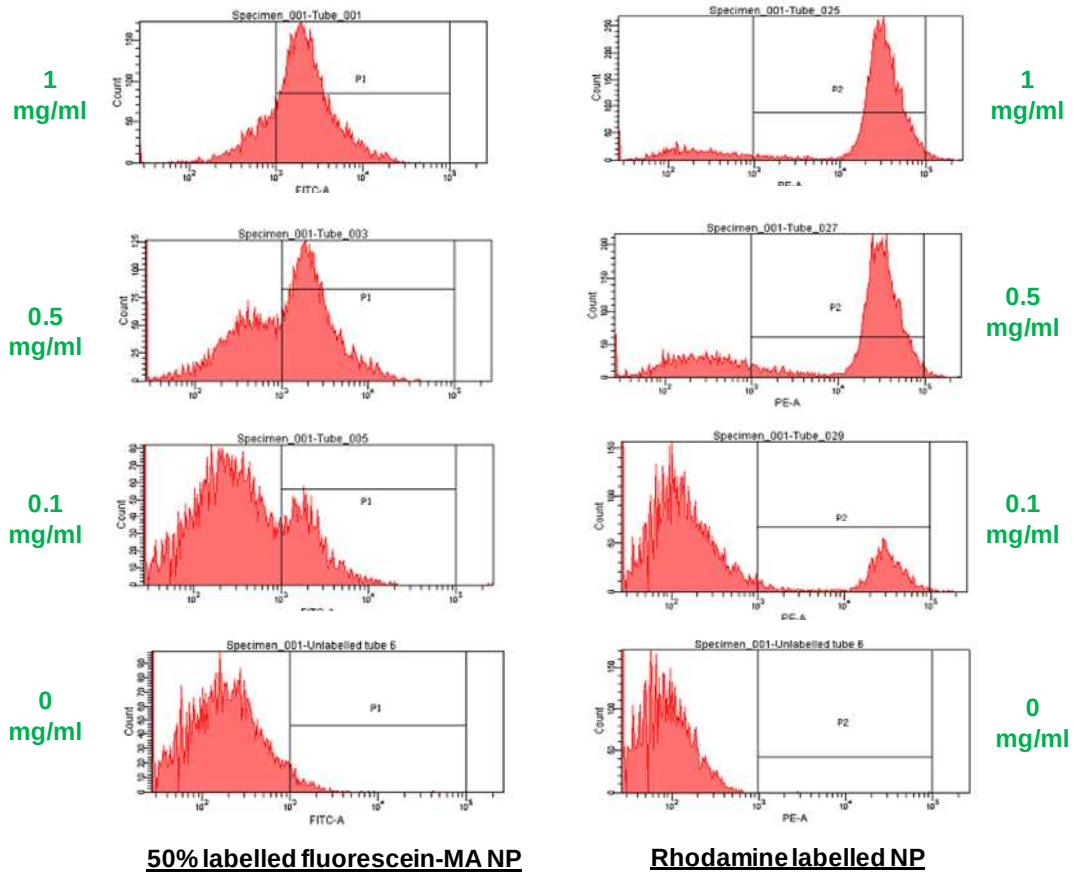

Figure 3.6 *Flow cytometry of nanoparticle uptake in THP-1 cell culture at increasing concentrations of Fluorescein -MA and rhodamine containing nanoparticles.*

When flow cytometry of nanoparticle uptake was measured on the macrophage cells pre-incubated individually with chemical inhibitors of endocytic pathways no inhibition was observed for any of the inhibitors used. Uptake was observed of the NPs similar to where no inhibitors were used. The specific inhibitors used were as described in section 3.5.4.3. No conclusion could therefore be drawn with flow cytometry regarding the mechanism of uptake of the nanoparticles.

3.6.5 Cell culture

The results obtained for the live and fixed cell imaging on the uptake of Fluorescein-MA NP studies was done to provide visual assessment of the uptake process and kinetics.

3.6.5.1 Nanoparticle uptake in U937 and THP-1 macrophages

All the results that are presented here are those of cells in their chemically differentiated state, which was achieved via treatment with PMA. Phorbol esters, such as PMA were reported to induce macrophage like differentiation in myelomonocytic and histiocytic luekaemic cell lines (e.g. THP-1 and U937) [179, 194].

The capability of macrophages to take up and accumulate the nanoparticles was investigated via confocal microscopy. The data as presented in figure 3.7 A and B illustrated that after treating the cells for an hour with 0.1 mg/ml Fluorescein-MA PLGA- or coumarin-PLGA-nanoparticles, the particles were visible within the cells and were thus successfully taken up into both the THP-1 and U937 macrophage cell lines, corroborating the flow cytometry results. Therefore including the MA into the nanoparticles did not affect the uptake into the macrophages negatively.

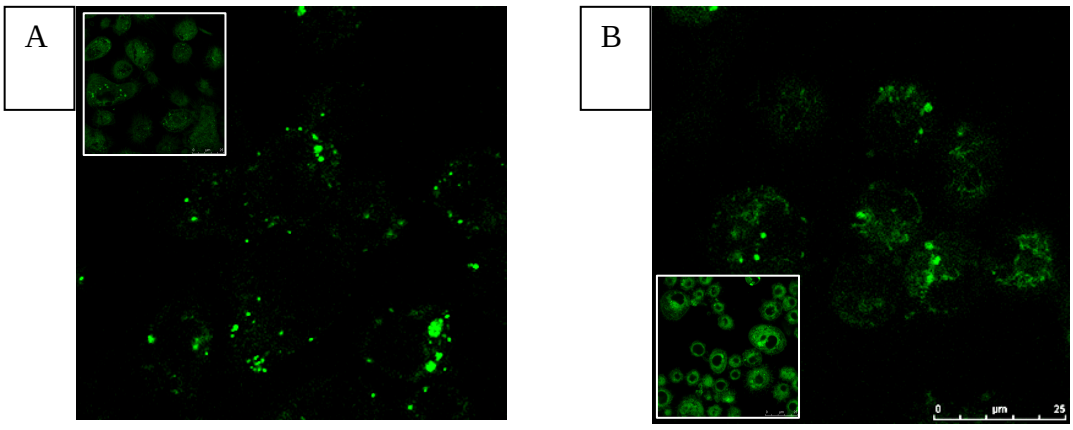

Figure 3.7 *Live cell images of Fluorescein-MA PLGA nanoparticles taken up by a) THP-1 and b) U937 macrophages. Inserts are controls i.e. coumarin labelled PLGA nanoparticles.*

For the effective design of clinically useful therapeutic molecules, it is necessary to understand the intracellular trafficking and fate of the molecules. To determine whether the nanoparticles reside within the early endosomes, initial co-incubation studies with Fluorescein-MA containing PLGA nanoparticles (green) and transferrin (red), with the transferrin representing early and recycling endosomes, was done for half an hour in the two different macrophage cell lines. The results (not shown) did not indicate co-localization. Whether the particles already moved through early endosomes or not could therefore not be concluded. To resolve this, pulse/chase studies were undertaken.

Interestingly, the coumarin PLGA particles were observed to affect the morphology of the macrophages. Light microscopy images (Figure 3.8) of THP-1 macrophages incubated either with unlabeled PLGA or coumarin labeled PLGA nanoparticles indicated that the coumarin PLGA treated cells (Figure 3.8A) yielded more flattened / less dense cells than the PLGA unlabeled treated cells. Whether coumarin PLGA serves as a good representative control as was used in literature is a point of contention [29]. It may be that in macrophage like cell lines the dye appears to be toxic whereas in other cell lines it is not [29]. It was decided not to use the coumarin labelled PLGA in the co-localization studies due to the coumarin most probably interfering with the metabolism of the cells.

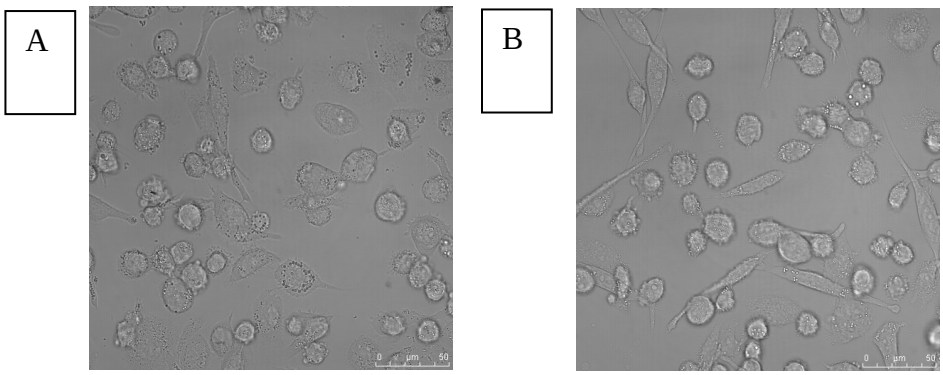

Figure 3.8 *Bright field confocal images of cell morphology of THP-1 macrophages after uptake of nanoparticles A) Coumarin PLGA B) unlabeled PLGA nanoparticles.*

Pulse/chase studies allow the determination of the path and end location of the nanoparticles within the cells after uptake. The endocytic probes (Figure 3.9) that were used were transferrin 633 or transferrin 488 and dextran alexa fluor 647, to represent early/recycling endosomes and late endosomes/lysosomes respectively. Dextran follows the route of early endosomes, through late endosomes reaching lysosomes [182]. Previous groups have shown that late endosomes and lysosomes are accessible to molecules in the plasma within 10-30 min. after uptake, with the half-life delivery of a fluid phase marker between 90 and 120 min. [182, 185, 195, 196].

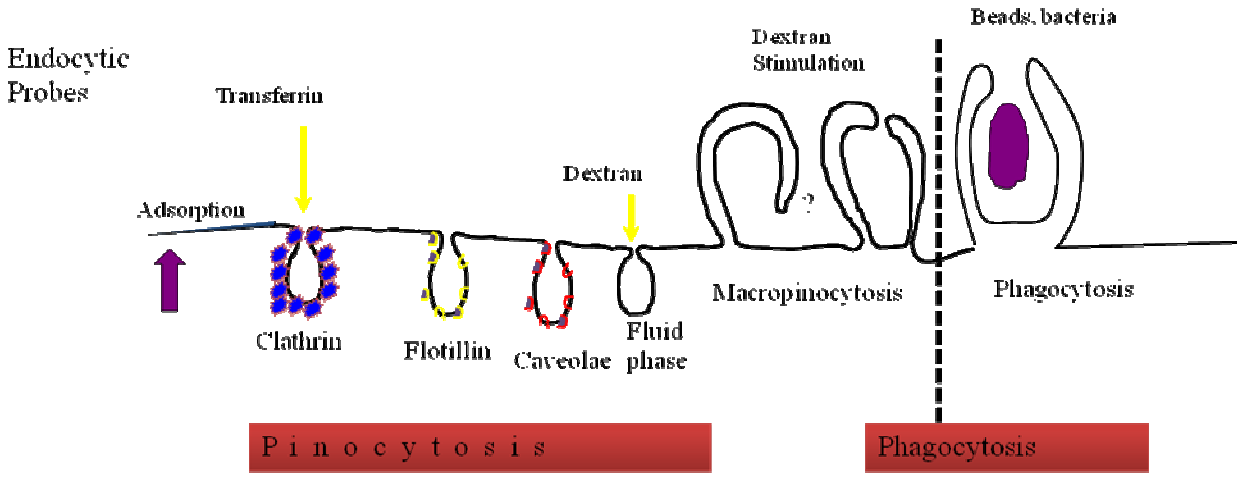

Figure 3.9 *Endocytic probes used for representation of endocytic pathways (Courtesy Dr. Arwyn T. Jones, Cardiff University, UK).*

In figure 3.10, the control experiment was done to show that the dextran positive compartments (late endosomes/lysosomes) were distinct from the early/recycling endosomes represented by transferrin-labelling. Z-stack imaging confirmed no-colocalization in areas where possible yellow spots were observed. The cells were treated with the nanoparticles at different time points as well as incubated with dextran or transferrin as indicated in figure 3.10

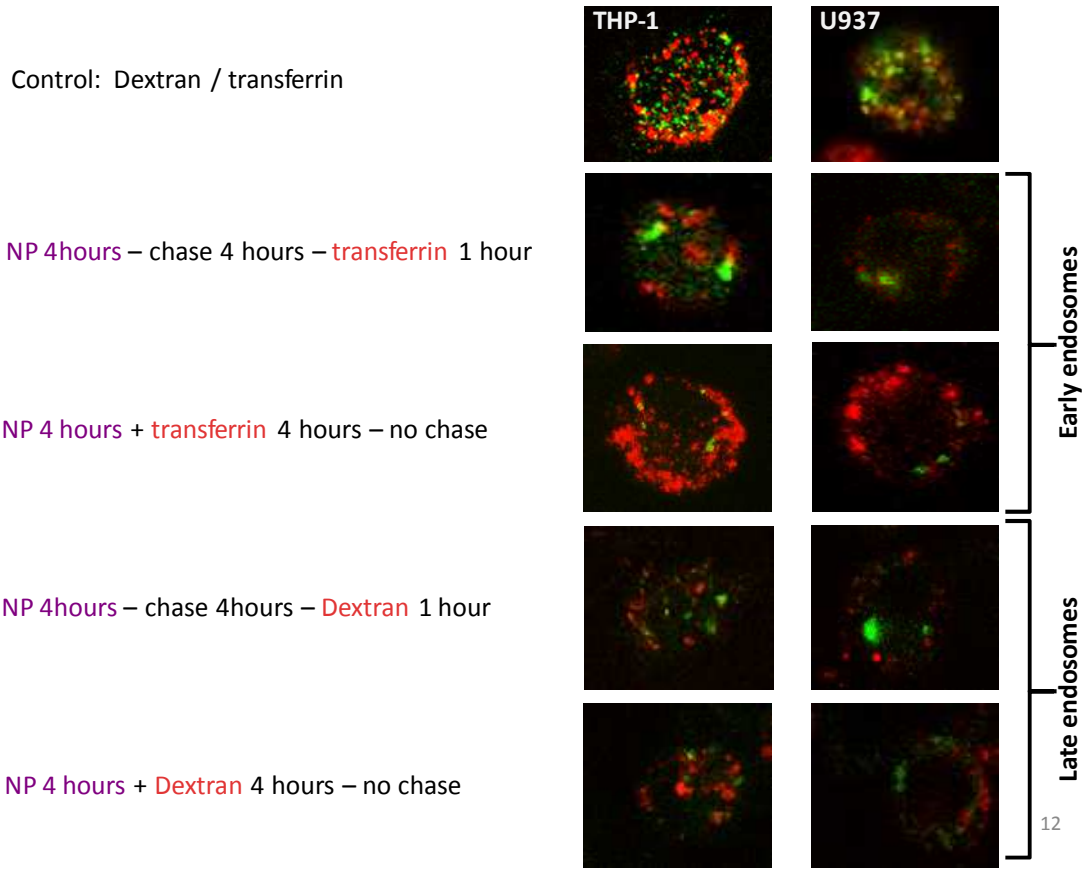

Figure 3.10 *Confocal images of intracellular processing of Fluorescein-MA using single sections through the macrophage cells of the pulse/chase experiments. The red stained regions represent either transferrin 633 or dextran alexa fluor 647. The green colours in the figures represent Fluorescein-MA PLGA nanoparticles. Yellow colours are indicative of co-localization.*

A summary for the transferrin 633 and the dextran alexa fluor 647 pulse/chase experiments with the nanoparticles is presented in the table 3.3

Table 3.3 Summary of figure 3.9 of pulse/chase studies that was conducted

	Observation:
Control:	
Dextran (red) 1 hour – chase – transferrin (green) 1 hour	No colocalization
Particles and transferrin:	
1. NP 4 hours – chase 4 hours – transferrin (red) 10 min	No colocalization
2. NP 4 hours – chase 4 hours – transferrin (red) 1 hour	No colocalization
3. NP + transferrin (red) 4 hours – no chase	Few areas of colocalization
Particles and Dextran:	
4. NP 4 hours – chase 4 hours – dextran (red) 1 hour	No colocalization
5. NP + dextran (red) 4 hours – chase 4 hours	No colocalization
6. NP + dextran (red) 4 hours – no chase 4 hours	No colocalization
7. Dextran (red)1 hour – chase 4 hours – NP 4 hours	No colocalization

The main reason why these pulse/chase experiments were done was to determine the endpoint location of the nanoparticles, and therefore without a chase step the nanoparticles could be at different stages of uptake (Figure 3.10 and table 3.3). When the study was done with the nanoparticles and transferrin, the only colocalization that was observed was when the nanoparticles and the transferrin were incubated together for 4 hours without a chase incubation step in between. This result could indicate that some of the particles might move through the recycling endosomes given the long incubation time of the transferrin, but no colocalization was observed in the early

endosomes by using this approach indicating that the nanoparticles have moved beyond the compartments which are represented by transferrin. It might be that the particles already passed through the early endosomes during the course of the longer incubation times used. The different pulse/chase studies with the nanoparticles and dextran did not show any colocalization indicating that the nanoparticles and the dextran are not localized in the same compartments of the cell. No co-localization was observed in these pulse/chase studies under the conditions used and it might be that the particles are already localized within the cytoplasm or other compartments.

3.6.5.2 Immunofluorescence staining of fixed macrophages

Because no conclusive results were obtained from the pulse/chase studies regarding the intracellular processing of the MA containing NPs after uptake, another approach was taken. The cells were treated with Fluorescein-MA PLGA nanoparticles for three hours, fixed and immunostained with different primary antibodies directed to specific cell organelles. As shown in figure 3.11, the early endosome antigen 1 marker (red) was used but did not show co-localization with the fluorescein-MA PLGA nanoparticles. The particles (green) in the image were confirmed to be present within the cells by z-stack imaging. The results correlate with that of figure 3.10, where with live cell imaging, co-localization with the early endosomes could also not be observed.

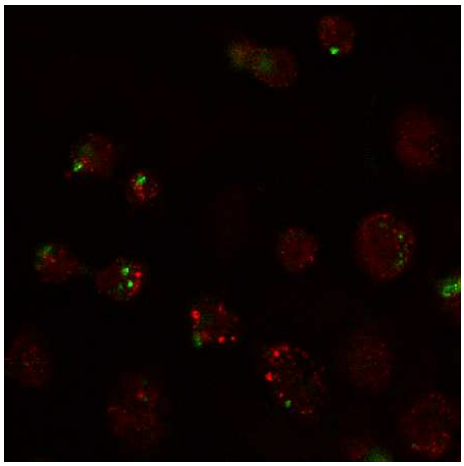

Figure 3.11 *Confocal imaging of possible colocalization of Fluorescein-MA PLGA (green) with primary antibody EEA1 (red) labelled organelles in THP-1 macrophage cells. Alexa fluor 633 secondary antibody stain was used to visualize the labelled organelles.*

Microscopic imaging was used to investigate two cytoskeletal inhibitors. Cytochalasin D was used to disrupt actin dependent pathways and nocodazole to disrupt the microtubule network. Attempts made with flow cytometry as discussed in section 3.6.4, showed that uptake took place regardless of several inhibitors used. Here confocal results indicated (figure 3.12) that Cytochalasin D treatment decreased uptake of the particles in both the THP-1 (shown) and U937 (not shown) cell lines. This suggests dependency of MA nanoparticles uptake on actin (red) and therefore microfilaments, at least in these cell lines. The illustration in figure 3.11A indicates intact actin networks and nanoparticles (green) within the cells, whereas in figure 3.11B a disrupted actin netork (red) together with particles present on the outside of the cell is visible. Nocodazole, which disrupts microtubules, treatment (not shown) did not have an effect on MA nanoparticle uptake in both the THP-1 and U937 cell lines.

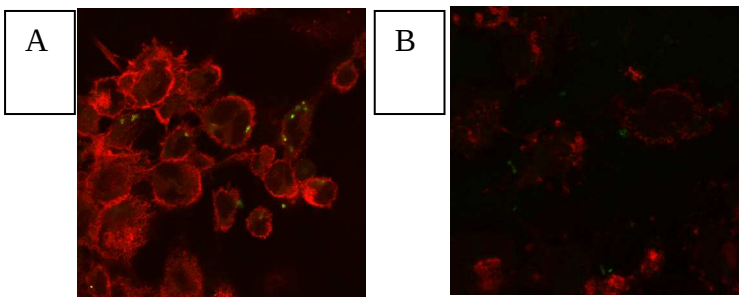

Figure 3.12 *Actin involvement in the uptake of Fluorescein-MA PLGA in THP-1 macrophage cells stained with rhodamine phalloidin for actin, a) No Cytochalasin D treatment, b) Treatment with Cytochalasin D.*

3.6.6 *In vitro* drug testing in *M.tb* H37Rv infected THP-1 macrophages

To determine the mycobactericidal activity of the INH containing nanoparticles compared to free INH, i.e. whether the drug is released from the nanoparticle, an *in vitro* infection study was performed where THP-1 macrophage cells were infected with *M.tb* H37Rv and used in the radiometric experiments as described in Methods [172]. A second aim was to determine whether the MA in the particles influences the efficiency of the *M.tb* inhibition. The radiometric experiments with the NPs containing INH and the free INH, were conducted at the same concentrations as for free INH (0.2 µg/ml and 2 µg/ml) so that the concentration of INH in the NP is the same as for the free INH.

The uptake of the particles was observed in THP-1 macrophage cells with previous confocal studies as discussed in section 3.6.5.1. The presumed advantage that the particles hold compared to the free drug is that due to its nanosize, intracellular uptake of the drugs will improve the availability of the drug to the intracellular bacteria. This was tested here. The effect of the inclusion into the nanoparticle of MA as targeting agent was tested here as well. The targeting advantage that may be gained by MA

inclusion was not tested, due to the absence of natural host anti-MA antibodies in the *in vitro* experimental design.

Infected macrophages were exposed to free INH and encapsulated INH with or without MA at different concentrations over 3 time points (5 hour, 1 day and 2 day exposures followed by an additional 2 day incubation time after washing the cells to remove particles and/or drugs that have not been taken up into the cells). After treatment with the different drugs and two days of incubation, the bacterial growth index (GI) was determined by means of the radiometric BACTEC 460 system. The bacteria were harvested for BACTEC by lysing macrophage cells with 0.1% Triton X-100. The results (figure 3.13) indicated the expected dose dependent effect of the drug on the inhibition of the growth of the bacteria. For the 5 hour treatment the standard deviations were too large to draw conclusions between the different test groups (results not shown). The 1 day and 2 day incubation time did show better growth inhibition compared to the 5 hour study compared to the nanoencapsulated INH, but was still not as effective as the free drug alone. The 2 µg/ml concentration of the nanoparticles was already out of range and showed just as good efficiency in the 1 and 2 day study as for the free drug alone.

It can be concluded from the results that the nanoencapsulation of INH results in a delay in drug release, possibly as a function of the polymer that slowly degrades in the macrophage. After 1 and 2 day exposure to the nanoencapsulated INH, significantly more inhibition was observed, but with reduced toxicity/efficiency compared to free INH. The effect of free INH on bacterial growth inhibition could be matched by using the higher concentration of 2 µg/ml of the nanoencapsulated INH with or without MA.

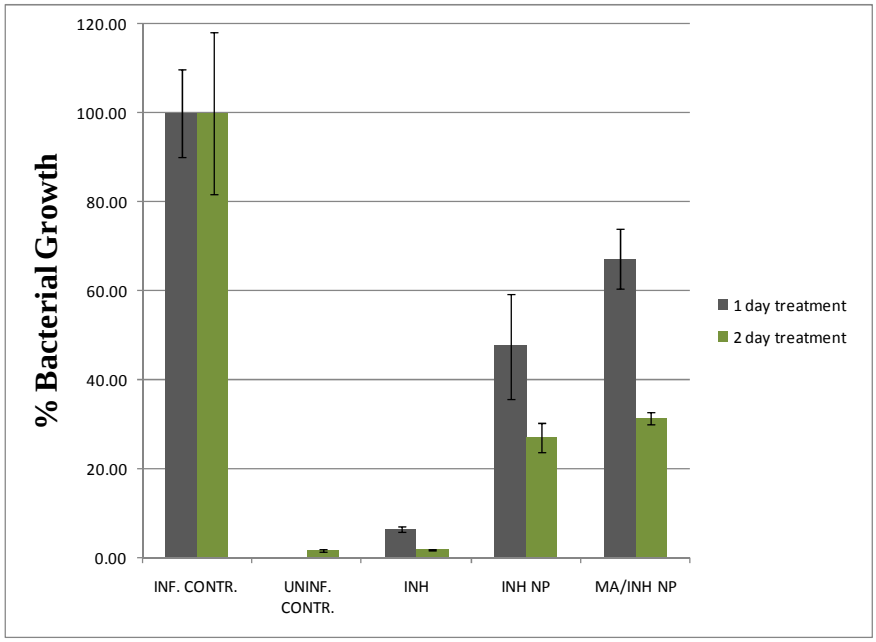

Figure 3.13 *The effect of nano-encapsulation of INH on its efficiency to suppress growth of M.tb in infected THP-1 macrophages using BACTEC. The results represent the average of triplicate values. Concentration for INH shown was 0.2µg/ml for free and encapsulated drug. The study with 2µg/ml INH was out of range. INF.CONTR = infected control, UNINF.CONTR = uninfected control, INH = isoniazid, INH NP = isoniazid containing nanoparticles, MA/INH NP = mycolic acid and isoniazid containing nanoparticles.*

In the *in vitro* model, the inclusion of MA in the INH nanoencapsulated particle did not show significant enhanced efficiency of delivery or toxicity of the INH drug in the macrophage. As the target for MA is represented by host antibodies to MA or concentrated spots of cholesterol, which were not present in the test, no significant difference in INH mycobactericidal efficiency was expected by the inclusion of MA in the nanoparticles. What was interesting to note was the fact that between the INH containing nanoparticles with and without MA incorporated, there was a statistical significant difference for both days ($P < 0.01$) where the INH in the MA NP had a lower efficiency compared to the INH in the NP without MA. It appeared as if the MA actually worked against INH in killing the *M.tb* in the macrophages. The observation that the MA inclusion actually worked against INH's bacterial inhibition, came as quite a surprise. This observation could be explained by the notion that the

MA might serve as an external source of the MA cell wall component, overcoming the bottleneck in cell wall synthesis during the proliferation cycle of *M.tb*.

The data further illustrates that INH was not incapacitated by the process of encapsulation, i.e. the double emulsion solvent evaporation freeze-drying technique, which involves shear forces and low temperatures. It further firmly confirmed that the nanoparticles are taken up by the macrophages and that INH is released from the particles, at the expected slower rate of release compared to the free drug.

3.7 Discussion

In the search for new or improved treatment against TB, nanoencapsulation of a known anti-TB drug was investigated here, including the use of a potential targeter to increase the efficiency of drug delivery to the site of infection. As mentioned before, controlled drug delivery devices such as nano and microparticles have numerous advantages compared to conventional dosage forms. Poly lactide-co-glycolide (PLGA) co-polymer, is a biodegradable and biocompatible polymer, that has often been used for controlled drug delivery systems, especially because of its non-immunogenic properties and having the capacity to encapsulate hydrophobic and hydrophilic agents [54]. As targeting agent, the mycobacterial cell wall component, MA from *M.tb* was investigated. MA has interesting biological activities, including foam cell formation and immune steering towards Th1 cellular responses [14, 126], as well as cholesteroid like properties [121]. The MA being present on the external surface of the nanoparticles may interact with anti-MA antibodies in the vicinity of the sites of infection to cause a localized immune complex that may enhance uptake of the NPs in the infected and surrounding uninfected macrophages. MA could also target cholesterol that is presumed to be concentrated around the sites of infection [81, 148] by means of its attraction to cholesterol [121]. By combining the possible targeting effect of MA to the infected cells and the slow release of the polymer, this approach was hypothesized to lead to effective TB treatment where the TB infected cells could be targeted and high intracellular concentrations of INH could be achieved.

The double emulsion-solvent evaporation freeze drying technique [55, 174] can be used for hydrophilic and hydrophobic drugs to be encapsulated in a polymer matrix [32, 60]. This method was applied to formulate nanoparticles of MA and INH into PLGA, a biocompatible and biodegradable polymer [34, 51, 55]. Successful encapsulation of 14% INH together with MA was achieved with the technique used, resulting in a negative zetapotential that may prevent unwanted agglomeration [32,

33]. The percentages of the INH and MA inside of the nanoparticles were not optimised for the purpose of these experiments.

The PLGA and MA-PLGA particles were found to be non-toxic to the mammalian host macrophage cells, compared to industrial nanoparticles [197]. This result supports literature indicating that amorphous silica, as was used in this study, is not toxic to cells [177] as well as Fe_2O_3 [175, 176]. The ZnO nanopowder which is toxic to cells, resulted in a significant reduction in cell viability as also described in literature [178].

The therapeutic effect of the drug loaded MA PLGA nanoparticles will greatly depend on the internalization and sustained retention in diseased cells. Although an *in vitro* system does not even remotely represent a highly evolved biological system, some preliminary data could be obtained to indicate the behaviour of the particles with the cells. THP-1 and U937 monocyte-macrophage like cell lines, which are often used in nanoparticle uptake studies [179, 198], were used to determine whether the labelled MA nanoparticles would be taken up by the cells. The data illustrated that labelled MA nanoparticles were successfully taken up into the two different macrophage cell lines which represent the target cells in the host. The results also indicated that the nanoparticles with an average size of 500 nm, a slightly negative zeta potential and a smooth external surface were appropriate for uptake by macrophage cell lines. This demonstrated that nanoparticles may serve as a suitable carrier for MA to reach their target sites.

These results of using PLGA in the formulation corroborate with examples in literature. PLGA microparticles were reported to be taken up specifically by macrophages of peritoneal exudate cells [32]. Hasegawa *et al*. also showed that RIF containing PLGA microparticles were phagocytosed in alveolar macrophages [186].

In another *in vivo* study it was also shown that PLGA microspheres containing trehalose dimycolate (TDM) were taken up by phagocytic cells [199].

The endocytic and intracellular trafficking routes are intricate and highly regulated to help mediate cellular homeostasis [185]. Knowledge of these complex systems could be used to better design and use nanoparticles for effective chemotherapy. After endocytic uptake, drug delivery systems could go into early sorting endosomes and recycling endosomes. Thereafter from early endosomes transported to late endosomes and finally to lysosomes [185]. In order to identify the intracellular compartments that the nanoparticles traverse, different endocytic markers were used. For live cell imaging transferrin was used to represent early / recycling endosomes. Transferrin binds to the transferrin receptor and is taken up by clathrin coated endocytosis, which then goes through the early and recycling endosomes, returning to the plasma membrane [182]. Dextran was used to represent late endosomes / lysosomal compartments because the molecule is taken up by fluid phase and then moves through early to late endosomes and finally to lysosomes [182].

In the pulse / chase experiments that determine the compartments the particles would occupy, it was observed that the nanoparticles only co-localized to a small extent with transferrin and not with dextran. From these results it was also observed that the endpoint of the nanoparticles was not the lysosomes. Whether they do pass through the lysosomes, remain to be determined. Live cell imaging, using short time intervals and different chase times are warranted to further elucidate particle trafficking. These results correlate with an *in vitro* uptake study done by Trombone and co-workers in peritoneal macrophages. They showed that no colocalization was observed with the marker dextran for PLGA microspheres containing TDM [199] even after 15 days of administration.

Another possibility is that the nanoparticles containing the MA reside within the cytoplasmic compartments of the cell as was previously illustrated for PLGA nanoparticles in human arterial smooth muscle cells (HASMC) by confocal and transmission electron microscopy experiments. The *in vitro* studies of Panyam *et al*. showed that endo-lysosomal escape occurred within 10 minutes through a process of surface cationization, where the particles associated with the wall of the endocytic vesicles before being released into the cytoplasm. Due to the acidic environment of the endo-lysosomes the particles had a cationic potential associating with the negatively charged membrane, leading to the particles' escape. The experiments also showed that the lysosomal vesicles stayed intact, possibly because of localized destabilisation and extrusion of the particles at the point of contact with the membrane [29]. If this applies to the present study as well, it might be that the MA containing nanoparticles can enter the cytoplasmic compartment of the cell soon after uptake. This property will be beneficial in drug delivery as the drug load in the particles will not be retained in the degradative environment of the lysosomal compartments in the cell but will rather be in the cytoplasmic compartment. MA incorporated into the PLGA nanoparticles could also contribute to the endocytic route that the nanoparticles might follow. As the coumarin labelled PLGA nanoparticles influenced the metabolism of the cells, no comparative studies were done to determine the effect the MAs would have on the nanoparticles localization within the cells. Another fluorescent label will be investigated in the future for comparative studies.

There are a number of obstacles in fluorescence microscopy when investigating endocytic trafficking. Live cell imaging does not allow for immuno-staining of intracellular structures and therefore fluorescent probes are used that also poses the challenge of concentration and pH dependent quenching that could be released from the carrier leading to misinterpretation of results. Traditional fixation methods could cause permeabilization of intracellular membranes allowing material to diffuse out leading to deceptive results. Both approaches are therefore applied to eliminate the possibility of fixation artefacts [185]. Here, fixation of the cells were done together with EEA1 (early endosomal antigen 1) antibody staining for early endocytic

structures. The Fluorescein-MA PLGA nanoparticles did not co-localize with EEA1, representing early endosomes, similar to the results obtained in the pulse/chase study with transferrin. One possibility could be that the particles might move through these compartments at a much faster rate as was intervalled for measurements in the actual experiments.

Preincubation of the cells with cytoskeletal inhibitors, before nanoparticle treatment, indicated an actin dependent uptake that could be inhibited by cytochalasin D. Nocodazole, which disrupts polymerization of microtubules and numerous endocytic processes [182, 200], did not have an effect on MA PLGA nanoparticle uptake. These results differ from a study done by Panyam and co-workers where the PLGA nanoparticles in HASMC cells were reported to be affected by Nocodazole and not by cytochalasin D [29]. But this could be due to the difference in size, as our particles are around 500 nm whereas the particles in the study of Panyam was around 70 nm in size, which also plays a role in the route of uptake. This could also point towards a difference in the reaction to chemical inhibitors [201] by the different cell lines used, or by the inclusion of MA that may affect the route of uptake and processing of the NPs. The main challenge here is that for every type of cell line the different inhibitors should be optimized and tested. The effect of uptake and processing inhibitors depends on the specific cell line used, as was shown in a report by Vercauteren *et al*. [201]. The authors showed that even poor specificity was observed in some cell lines. Thus the optimized concentrations obtained in literature [140, 182, 183] can only be used as a guideline. Optimization of inhibitor concentrations for the specific cell lines used in this study, with rigorous controls in place, may yield more data on the mechanism of uptake and processing of MA containing NPs.

The efficacy of the free vs encapsulated drugs were tested with *M.tb* infected macrophage cells over a period of 4 days. A 5 hour incubation of nanoparticles was less effective compared to the 1 and 2 day exposures to kill the mycobacteria as was to be expected due to the slow degradation rate [58] of the nanoparticles and the

probability that the INH remains associated to the polymer during the degradation. The indication of a reduction in the bacterial growth in the NP-INH-MA treated macrophages confirmed uptake of the nanoparticles into the TB infected cells and the subsequent release of the drug from the polymer.

Although the encapsulated INH appeared to be less effective compared to the free drug, it might be that the INH is still associated with the polymer in an environment where the polymer is not degraded as efficiently as would be the case in a physiological environment. Comparing the rate of degradation of PLGA microspheres in an *in vivo* vs an *in vitro* environment in literature, it was shown that the *in vivo* degradation was much faster (1.7-2.6 times) than that *in vitro,* in buffer at physiological pH and temperature, regardless of the end group or molecular weight of the PLGA. The faster degradation might be due to several factors, such as free radical formation and acid or enzymatic products formed by the host's immune cells that could enhance the degradation process that is not present in an *in vitro* environment [58]. As mentioned previously, PLGA microparticles have been shown to be taken up by macrophage cells even without targeting ligands. Therefore it is envisioned that the effective dose required *in vivo* would be much less than the free drug that is able to traverse to different areas in the host in contrast to what was observed in the *in vitro* experiments.

A number of research groups are currently investigating the use of nanodrug delivery vehicles to enhance the efficacy of anti-TB drugs. The research group of Khuller and co-workers have been analysing a number of different delivery vehicles to enhance the efficiency of existing anti-TB drugs. They tested the use of solid lipid inhalable particles for the first line anti-TB drugs, where they could reduce the number of administrations required by more than 6-fold [50]. The group also showed that inhalable alginate nanoparticles were detectable for up to 15 days in organs [202-204], and that PLGA microparticles have a sustained release over several days [205]. The frequency of dose administration could also be reduced by making use of carrier

systems. In a guinea pig model it was shown that the treatment frequency could be reduced 9-fold by encapsulating RIF or INH into PLGA nanoparticles due to the sustained slow release of the drugs from the carrier vehicle [206]. The results shown in literature, as mentioned above for PLGA polymers as carrier vehicle, support sustained release and the possibility of enhanced uptake in the macrophages without the use of targeting ligands. The contribution that our research is able to make is in the region of specific targeting. The uptake of drugs by infected macrophages would not only be enhanced by the synthetic PLGA polymer carrier vehicle but also by the presence of MA that may facilitate opsonisation of the nanoparticles for macrophage uptake mainly at the site of MA antigen production. In addition, the cholesteroid nature of MA and its ability to bind cholesterol could also cause a physical attraction to the cholesterol rich sites of persistent *M.tb* infection.

This study is the first to report encapsulation of MA into solid matrix PLGA nanoparticles together with anti-TB drugs. *In vitro* experiments did show successful uptake into macrophages. The localization fate of the NPs within the cells still needs to be confirmed. Because the studies done by Panyam *et al*. did indicate that the PLGA particles ended up within the cytoplasm, the predictions are that our PLGA nanoparticles will also preferentially occupy the cytoplasm [29]. The inclusion of the MA into the PLGA nanoparticles did not reduce the efficiency of uptake into the macrophage cells, as indicated with flow cytometry and confocal imaging, although the mechanism of uptake and processing in the cells could not be concluded with the results obtained. A requirement for the actin cytoskeleton was observed when the cells were treated with cytochalasin D and visualized with confocal microscopy. Actin plays a role in various different uptake mechanisms such as clathrin dependent endocytosis and macropinocytosis [51, 207].

The BACTEC experiments confirmed a slow release of the anti-TB drug from the polymer. The inclusion of MA into the nanoparticles seemed harmless to the host macrophages, but decreased the mycobactericidal efficiency of INH somewhat, an observation that may possibly be attributed to INH inhibiting the natural MA

biosynthesis of the pathogen, while inclusion of MA in the NP adds an external source of this metabolite to the pharmacologically stressed *M.tb*.

The system is now ready to be tested *in vivo*, where the efficiency of MA as a targeting agent may be assessed. It is envisaged that the MA will firstly serve as an antigen that forms immune-complexes with anti-MA antibodies, which universally occur in all TB patients [120]. This may facilitate opsonisation of the nanoparticles for macrophage uptake mainly at the site of infection, where the mycolic acid antigen is naturally produced and released. Secondly, because of the cholesteroid and cholesterophilic nature of MA [121], it may in effect be attracted to the anticipated cholesterol rich sites of *M.tb* infection.